

## **Alternative electron pathways of photosynthesis drive the algal CO<sub>2</sub> concentrating mechanism**

Adrien Burlacot<sup>\*</sup>, Ousmane Dao, Pascaline Auroy, Stephan Cuiné, Yonghua Li-Beisson, Gilles Peltier<sup>+</sup>

Aix Marseille Univ, CEA, CNRS, Institut de Biosciences et Biotechnologies Aix-Marseille, CEA Cadarache, 13108 Saint-Paul-lez-Durance, France

<sup>\*</sup> present address: Howard Hughes Medical Institute, Department of Plant and Microbial Biology, 111 Koshland Hall, University of California, Berkeley, CA 94720-3102 USA

<sup>+</sup>: correspondence to Gilles Peltier ([gilles.peltier@cea.fr](mailto:gilles.peltier@cea.fr))

**ORCID IDs:** 0000-0001-7434-6416 (A.B.), 0000-0002-7040-5770 (O.D.); 0000-0002-3376-6550 (P.A.), 0000-0002-3000-3355 (S.C.), 0000-0003-1064-1816 (Y.L.-B.), 0000-0002-2226-3931 (G.P.)

**Author contributions:** A.B. and G.P. designed the research; A.B., O.D., P.A., S.C., and G.P. performed research; A.B. and G.P. contributed new reagents/analytic tools; A.B. and G.P. analyzed data; A.B. and G.P. wrote the paper with inputs from Y.L.-B.

**One sentence summary:** Photosynthetic alternative electron flows and mitochondrial respiration drive the algal CO<sub>2</sub> concentrating mechanism

**Key words:** bioenergetics, CO<sub>2</sub> mitigation, CO<sub>2</sub> concentrating mechanism, cyclic electron flow, microalgae, non-photochemical quenching, O<sub>2</sub> photoreduction, photosynthesis, flavodiiron proteins

## Abstract

Global photosynthesis consumes ten times more CO<sub>2</sub> than net anthropogenic emissions, and microalgae account for nearly half of this consumption<sup>1</sup>. The great efficiency of algal photosynthesis relies on a mechanism concentrating CO<sub>2</sub> (CCM) at the catalytic site of the carboxylating enzyme RuBisCO, thus enhancing CO<sub>2</sub> fixation<sup>2</sup>. While many cellular components involved in the transport and sequestration of inorganic carbon (C<sub>i</sub>) have been uncovered<sup>3,4</sup>, the way microalgae supply energy to concentrate CO<sub>2</sub> against a thermodynamic gradient remains elusive<sup>4-6</sup>. Here, by monitoring dissolved CO<sub>2</sub> consumption, unidirectional O<sub>2</sub> exchange and the chlorophyll fluorescence parameter NPQ in the green alga *Chlamydomonas*, we show that the complementary effects of cyclic electron flow and O<sub>2</sub> photoreduction, respectively mediated by PGRL1 and flavodiiron proteins, generate the proton motive force (*pmf*) required by C<sub>i</sub> transport across thylakoid membranes. We demonstrate that the trans-thylakoid *pmf* is used by bestrophin-like C<sub>i</sub> transporters and further establish that a chloroplast-to-mitochondria electron flow contributes to energize non-thylakoid C<sub>i</sub> transporters, most likely by supplying ATP. We propose an integrated view of the CCM energy supply network, describing how algal cells distribute photosynthesis energy to power different C<sub>i</sub> transporters, thus paving the way to the transfer of a functional algal CCM in plants towards improving crop productivity.

## Introduction

In aquatic ecosystems, microalgal photosynthesis has to cope with a low CO<sub>2</sub> availability resulting from the slow diffusion of CO<sub>2</sub> in water<sup>7</sup>. Moreover, the CO<sub>2</sub>-fixing enzyme Ribulose-1,5-Bisphosphate Carboxylase-Oxygenase (RuBisCO) has a low affinity for CO<sub>2</sub><sup>8</sup>, thus the efficiency of algal photosynthesis strongly relies on a CO<sub>2</sub>-Concentrating Mechanism (CCM)<sup>9</sup>. The algal CCM involves the sequential actions of inorganic carbon (C<sub>i</sub>) transporters and carbonic anhydrases located in different cellular compartments<sup>10</sup>, and results in active accumulation of CO<sub>2</sub> at the RuBisCO level<sup>4,6</sup>. Several CCM components have been identified in the green alga *Chlamydomonas reinhardtii* (*Chlamydomonas* hereafter)<sup>3,4</sup>, particularly putative C<sub>i</sub> transporters operating across the plasma membrane (High Light Activated 3, HLA3)<sup>11</sup>, the chloroplast envelope (Low Carbon Inducible A, LCIA)<sup>12,13</sup>, and more recently across the thylakoid membrane (bestrophin-like transporters, BSTs)<sup>14</sup>. The transport of C<sub>i</sub> across membrane bilayers against a concentration gradient is an energy-dependent process<sup>6,14</sup>, and the role of photosynthesis in supplying the chemical energy required by the functioning of CCM has been early recognized<sup>15</sup>.

During photosynthesis, sunlight is converted into chemical energy by two photosystems (PSII and PSI) acting in series through the so-called Linear Electron Flow (LEF), reducing NADP<sup>+</sup> into NADPH and producing a *pmf* across the thylakoid membrane. The *pmf* is then used for ATP synthesis, and both NADPH and ATP supply energy for CO<sub>2</sub> fixation. However, LEF produces less ATP than required for CO<sub>2</sub> fixation as compared to NADPH<sup>16</sup>, and photosynthesis relies on additional mechanisms to fill this gap<sup>17</sup>. These include *i.* cyclic electron flow around PSI (CEF), which involves both Proton Gradient Regulation-5 (PGR5)<sup>18,19</sup> and Proton Gradient Regulation Like-1 (PGRL1) proteins in plants and algae<sup>20,21</sup> and *ii.* pseudo-cyclic electron flow (PCEF) which diverts electrons to O<sub>2</sub> at the PSI acceptor side<sup>22</sup>, catalyzed by flavodiiron proteins (FLVs) in cyanobacteria<sup>23</sup>, bryophytes<sup>24,25</sup> and green microalgae<sup>26</sup>. Both CEF and PCEF generate a *pmf* without producing NADPH, thus re-equilibrating the high NADPH/ATP ratio of LEF. Another pathway involving several metabolic shuttles between chloroplast and mitochondrial respiration, called here chloroplast-to-mitochondria electron flow (CMEF), can also supply extra ATP for CO<sub>2</sub> fixation when CEF is absent or deficient<sup>27,28</sup>. In this context, how photosynthesis energy is delivered to the different C<sub>i</sub> transporters and how can this be done without compromising CO<sub>2</sub> fixation capacity are pivotal questions<sup>4,6</sup>.

In this work, we addressed these questions by studying *Chlamydomonas* mutants of CEF (*pgrl1*<sup>21</sup>), PCEF (*flvB*<sup>26</sup>) and of the recently discovered thylakoid C<sub>i</sub> transporters BSTs<sup>14</sup>. We show that CCM activity is unaffected in the single CEF or PCEF mutants but severely impaired

in the double mutants and that the trans-thylakoid *pmf* produced by the cooperative action of these mechanisms is used by BST thylakoid  $C_i$  transporters. We further establish that CMEF is involved in CCM functioning, most likely by supplying ATP to plasma membrane and/or chloroplast envelope  $C_i$  transporters, thus revealing how transport steps distant from the thylakoid can be empowered.

## Results

**Combined deletion of FLVs and PGRL1 impairs  $C_i$  affinity and growth in air.** To investigate the involvement of FLV-mediated PCEF and PGRL1-mediated CEF in the energy supply to the CCM, we first measured net photosynthetic  $O_2$  production at various  $C_i$  concentrations in *Chlamydomonas flvB*<sup>26</sup> or *pgrl1*<sup>21</sup> single mutants. When cells were grown under air (400 ppm  $CO_2$ , low  $CO_2$ ),  $C_i$  affinities were similar for control WT strains and single mutants ( $K_{1/2} \sim 10 \mu M$ ), indicating a fully functional CCM (**Fig. 1 A, B, H**). Under high  $CO_2$  (3%  $CO_2$  supplementation to air), *flvB* and *pgrl1* mutants as well as their respective progenitors showed similar affinity for  $C_i$  with a  $K_{1/2}$  around 100  $\mu M$  (**Fig. 1 D, E, H**). In order to assess possible functional redundancy between FLVs and PGRL1, double mutants were obtained by genetic crosses of the single *pgrl1* and *flvB* mutants (**Extended data Fig. 1 A**). Among the progenies, five independent double mutants were isolated (*pgrl1 flvB*-1, 2, 3, 4 and 5) as well as four independent control strains exhibiting normal accumulation of both FLVs and PGRL1 (thereafter called WT-1, 2, 3 and 4) (**Fig. 1 G; Extended data Fig. 1**). While no difference in  $C_i$  affinities was observed between these strains when grown at high  $CO_2$ , double mutants showed a 7 times lower affinity for  $C_i$  as compared to control strains when grown at low  $CO_2$  (**Fig. 1 C, F, H; Extended data Fig. 2 B, D**).

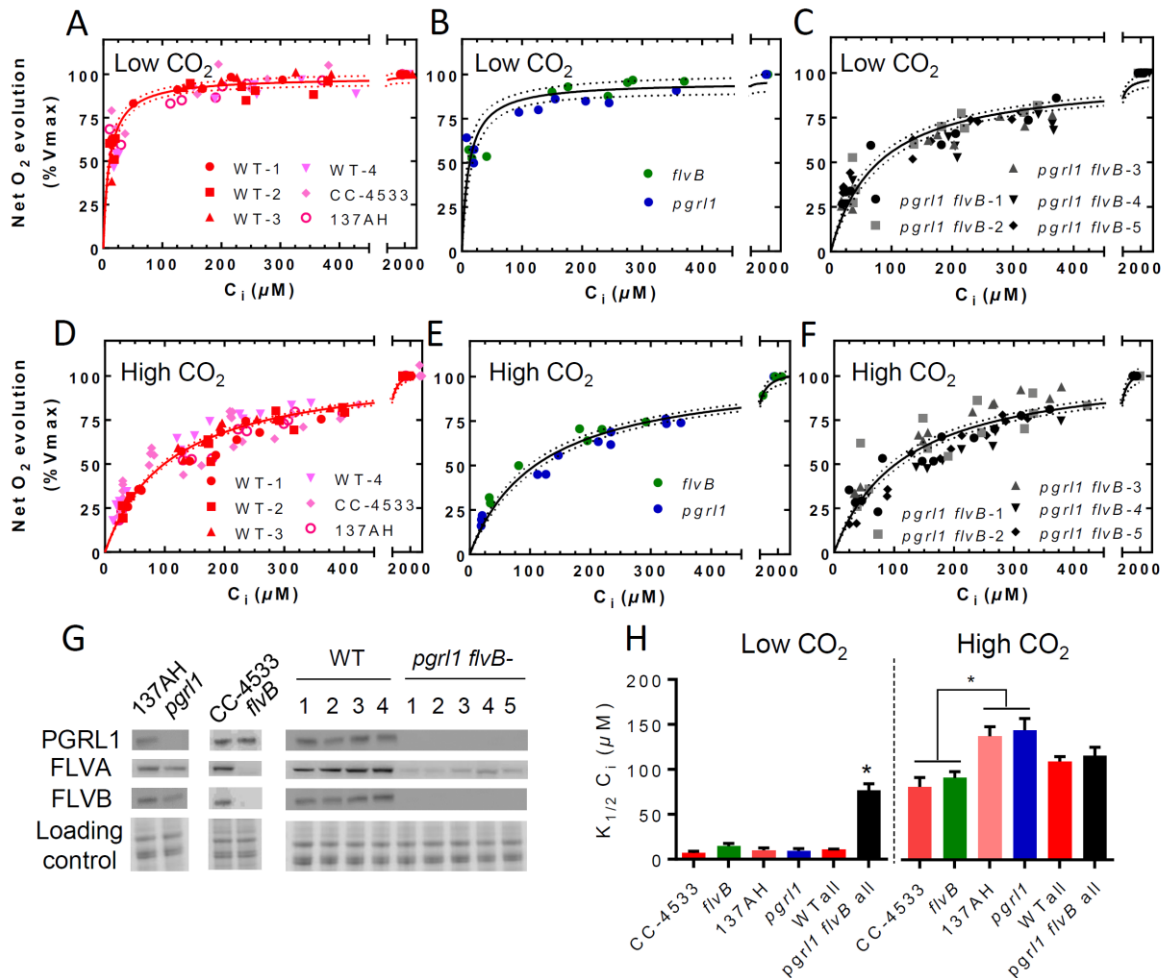


**Figure 1. Affinity of photosynthetic O<sub>2</sub> evolution for inorganic carbon (C<sub>i</sub>) is decreased in *pgrl1 flvB* double mutants, but unaffected in *flvB* and *pgrl1* single mutants.** Net O<sub>2</sub> production was measured at pH 7.2 in cells grown under 400 ppm CO<sub>2</sub> air (Low CO<sub>2</sub>) (A, B and C) or 3% CO<sub>2</sub> (High CO<sub>2</sub>) (D, E and F). Shown are three replicates for each strain (dots) and hyperbolic fit with variability (plain lines, dotted lines). For each replicate, net O<sub>2</sub> production was measured following stepwise C<sub>i</sub> addition, and normalized to the maximum photosynthetic net O<sub>2</sub> production. Since these strains were generated in different genetic backgrounds (CC-4533 and 137AH, respectively) showing contrasted photosynthetic activities (**Extended data Fig. 2 A, C**), data shown are normalized to the maximal net O<sub>2</sub> production rate. (A, D) 137AH and CC-4533 are the respective control strains for *pgrl1* and *flvB*, WT-1 to -4 are four independent control strains obtained from the *pgrl1* × *flvB* crossing. (B, E) *flvB* and *pgrl1* mutant strains. (C, F) *pgrl1 flvB*-1 to -5 are five independent double mutant strains. G Immunodetection of PGRL1, FLVA and FLVB in the different strains with Coomassie blue staining as the loading control. (H) K<sub>1/2</sub> C<sub>i</sub> values as determined from the hyperbolic fit for each strain. Shown are mean ± SD (n=3 for single mutants and their controls), values for all double mutant strains have been pooled (“*pgrl1 flvB* all”, n=15) as well as their control strains (“WT all”, n=12). Asterisks represent significant differences (p<0.05, one way ANOVA with Tukey correction).

Mutants defective in the CCM often cannot grow properly in low CO<sub>2</sub>. Here, we compared growth at different CO<sub>2</sub> concentrations, pH and light intensities. While all strains showed similar growth at high CO<sub>2</sub>, the growth of *pgrl1 flvB* double mutants was impaired under low CO<sub>2</sub> and very low CO<sub>2</sub> (100 ppm CO<sub>2</sub> in air) (**Fig. 2 A**), similar to the growth defect observed in the CCM-deficient mutant *cia5* (**Fig. 2 A; Extended data Fig. 3**). The growth defect observed in double mutants worsened with light intensity but was barely affected by pH (**Extended data Fig. 3**). The accumulation of the major CCM components, as evaluated by immunodetection, was similar in all strains, with the exception of LCII which is present in lower amount in double mutants (**Fig. 2 B**) and to a lesser extent in single mutants (**Extended data Fig. 4 C**). Since growth of the LCII knock-out mutant was shown to be not affected by low CO<sub>2</sub><sup>29</sup>, we conclude however that the *pgrl1 flvB* mutants growth defect is not due to the lower LCII level. Carbonic anhydrase activity measured *in vivo* was induced in low CO<sub>2</sub> reaching similar levels in all strains (**Fig. 2 C**). Double mutants and control strains showed similar maximal O<sub>2</sub> photosynthetic production (**Extended data Fig. 2 A, C**) and PSII quantum yields (**Extended data Fig. 4 A**), as well as similar levels of major photosynthetic complexes (**Extended data Fig. 4 B**). We conclude from these experiments that PGRL1-mediated CEF and FLV-mediated PCEF contribute to the CCM operation likely by supplying energy, and can compensate each other, as exemplified by the absence of phenotype in single mutants.

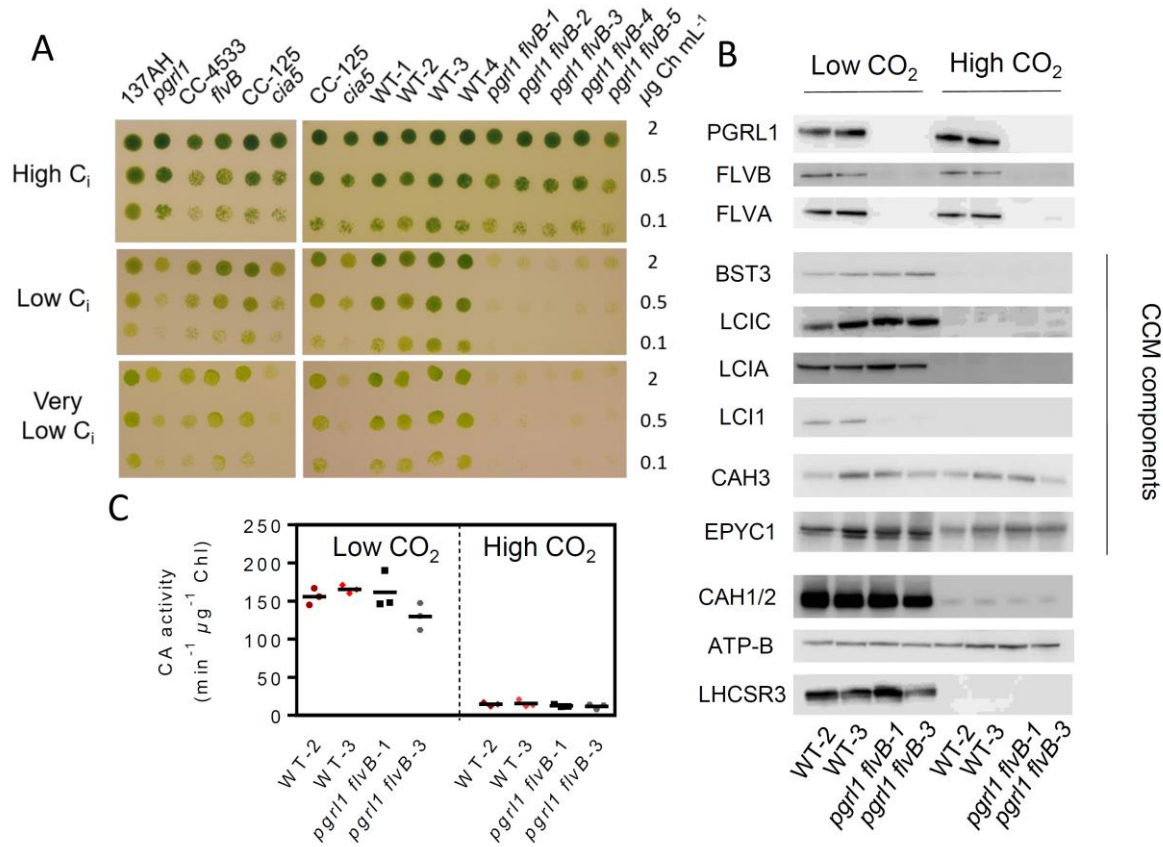


**Figure 2. Growth of *pgrl1 flvB* double mutants is impaired at low  $CO_2$  while CCM components are present. (A).** Growth tests performed on *pgrl1*, *flvB*, and their corresponding control strains (137AH and CC-4533 respectively) (left panels) and on double mutants (*pgrl1 flvB*-1 to -5) and their control strains (WT-1 to -4) (right panels); the CCM1 mutant *cia5* was introduced as a CCM-deficient control together with its reference strain CC-125. Cells were spotted on plates containing minimal medium at pH 7.2 and grown under continuous illumination ( $60 \mu\text{mol photon m}^{-2} \text{s}^{-1}$ ) either under High  $CO_2$ , Low  $CO_2$  or Very Low  $CO_2$  (100 ppm  $CO_2$  in air). Shown are representative spots of ten independent experiments. **(B)** Immunodetection of PGRL1, FLVA, FLVB and of the major CCM components in two independent *pgrl1 flvB* double mutants and controls grown in Low  $CO_2$  or High  $CO_2$ . **(C)** Carbonic anhydrase (CA) activity was determined *in vivo* by following the unlabelling of  $^{18}O$ -enriched  $CO_2$  in the same strains and conditions as in **B**. Shown are mean values and replicates (n=3).

**The *pmf* generated by CEF and PCEF energizes the CCM at the level of  $C_i$  transport across the thylakoid membrane mediated by BSTs.** To gain further insight into the link between CEF, PCEF and CCM energization, we assessed the level of the *pmf* dynamics across the thylakoid membranes in the different mutant strains during the functioning of the CCM. Currently, no direct measurement of *pmf* is available, but it can be inferred by the level of the rapidly reversible non-photochemical-quenching component (qE). The Light-Harvesting Complex Stress-Related 3 protein (LHCSR3), responsible for qE is activated by low luminal pH, making qE a sensitive and reliable probe of luminal pH<sup>30,31</sup> (**Fig. 3 A**). We thus took advantage of the presence of LHCSR3 in low CO<sub>2</sub>-grown cells (**Fig. 2 B, Extended data Fig. 4 C**) to quantify the luminal pH and the *pmf*. In both control lines and single mutants, the NPQ level was maximal when  $C_i$  level was low, and rapidly and reversibly decreased either in the light upon  $C_i$  injection or at low  $C_i$  when light was turned off (**Fig. 3 B; Extended data Fig. 5 A-E, I**). In sharp contrast, no CO<sub>2</sub>-dependent NPQ could be observed in the *pgrl1 flvB* mutants (**Fig. 3 C; Extended data Fig. 5 F, J**) where only a slowly inducible and irreversible NPQ was observed. We conclude from this experiment that CEF and PCEF energize the CCM through the generation of a trans-thylakoidal *pmf*, both mechanisms being able to substitute for each other.

Recently, three BST-like proteins were proposed to transport  $C_i$  at the thylakoid level<sup>14</sup>. To gain insight into the role of the *pmf* in the supply of energy to BSTs, we assessed the kinetics of the  $C_i$ -dependent NPQ in a BST knock-down strain (*bsti-1*)<sup>14</sup>. While the control strain showed a  $C_i$ -dependent NPQ (**Fig. 3 D**), the NPQ of *bsti-1* was barely affected during  $C_i$  depletion (**Fig. 3 E; Extended data Fig. 5 G, H**), thus indicating that the *pmf* is not consumed during  $C_i$  depletion in the *bsti-1* mutant. The low NPQ levels in *bsti-1* are attributable here to the lower accumulation of LHCSR3 as compared to its control strain (**Extended data Fig. 4 D**). We conclude from this experiment that the *pmf* generated by CEF and PCEF is used by BST proteins to transport  $C_i$  across the thylakoid membranes (**Fig. 3 A**).



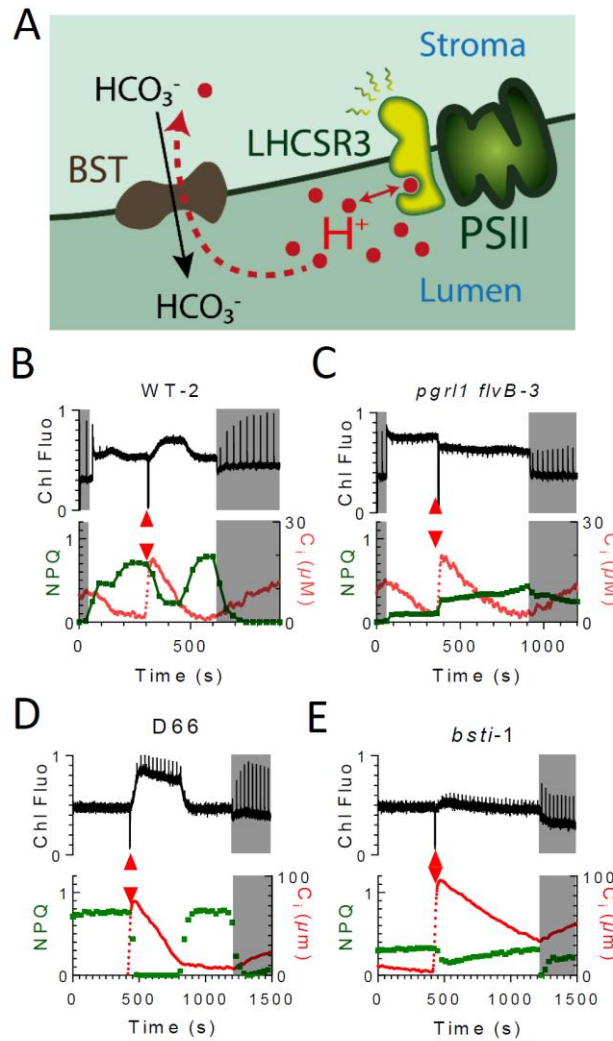


**Figure 3. The NPQ dependence to  $C_i$  concentration is abolished in *pgr1 flvB* double mutants and in the BST mutant *bsti-1*.** (A) Schematic view describing the rationale of the experiment; NPQ, which depends on the luminal pH (via LHCSR3) is used to probe the trans-thylakoidal *pmf* during the CCM functioning. (B-E) Combined measurements of chlorophyll fluorescence (upper panels),  $C_i$  concentrations and NPQ (lower panels) during dark-light-dark transients in WT-2 (B), *pgr1 flvB-3* (C), the *bsti-1* control strain D66 (D) and *bsti-1* (E). All strains were grown at low  $\text{CO}_2$ . Shown are representative experiments ( $n=3$ ). Red arrows indicate addition of bicarbonate.

**CMEF is the third protagonist of the triumvirate.** In order to gain quantitative insight into the nature of compensation mechanisms in *pgr1*, we investigated the  $C_i$  dependence of the light-dependent  $\text{O}_2$  consumption measured using  $^{18}\text{O}$ -labelled  $\text{O}_2$ . As previously reported<sup>32,33</sup>,  $\text{O}_2$  consumption increased at low  $C_i$  in control strains (Extended data Fig. 6 A, E). In *pgr1*,  $\text{O}_2$  uptake rates were higher than in control strains (Extended data Fig. 6 A-D), which was

previously attributed to an increase of the FLV-mediated PCEF<sup>27</sup>. O<sub>2</sub> uptake rates were strongly diminished in *flvB*<sup>26</sup>, but surprisingly, a C<sub>i</sub>-dependent O<sub>2</sub> uptake process remained (**Extended data Fig. 6 E, F**). In order to determine whether mitochondrial respiration is responsible for the remaining light-dependent O<sub>2</sub> uptake, we used two mitochondrial respiration inhibitors, myxothiazol and salicyl hydroxamic acid (SHAM), which inhibit the cytochrome *bc*<sub>1</sub> complex and the mitochondrial alternative oxidase, respectively. We show that the remaining light-dependent O<sub>2</sub> uptake measured at low C<sub>i</sub> in *flvB* is indeed due to mitochondrial respiratory activity driven by photosynthesis and therefore attributed to CMEF (**Extended data Fig. 6 K**).

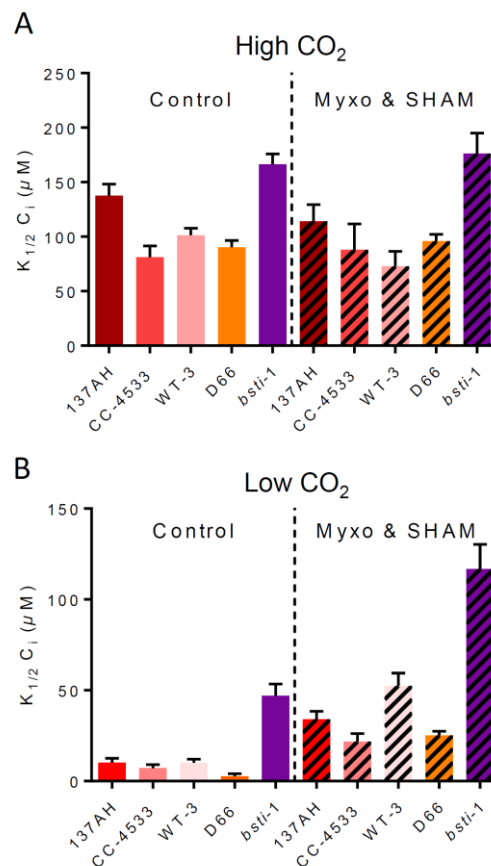


**Figure 4. Mitochondrial inhibitors decrease the affinity of photosynthesis for C<sub>i</sub> in low CO<sub>2</sub>-grown cells.** Photosynthetic net O<sub>2</sub> production was measured as in **Fig. 1** in High CO<sub>2</sub> (**A**) or Low CO<sub>2</sub> (**B**) grown cells. K<sub>1/2</sub> values were determined from hyperbolic fits in the different strains in the presence or absence of two mitochondrial inhibitors myxothiazol (Myxo, 2.5 µM) and salicyl hydroxamic acid (SHAM, 400 µM), respectively acting on the cytochrome *bc*<sub>1</sub> complex and on the alternative oxidase. Shown are mean values (n=3, ±SD). All strains showed K<sub>1/2</sub> significantly different when treated with myxothiazol and SHAM as compared to their control when grown in low CO<sub>2</sub> (p<0.05; one way ANOVA with Tukey correction).

We then investigated the contribution of mitochondria to CCM energization in wild-type strains. While addition of respiratory inhibitors had no effect on the  $V_{\text{Max}}$  and  $C_i$  affinity of high  $\text{CO}_2$ -grown strains ( $K_{1/2} \sim 100 \mu\text{M}$ ) (**Fig. 4 A, Extended data Fig. 7 D-F, I**), it reduced by half the  $C_i$  affinity of low  $\text{CO}_2$ -grown control strains ( $K_{1/2} > 20 \mu\text{M}$ ) as compared to untreated cells ( $K_{1/2} \sim 10 \mu\text{M}$ ) (**Fig. 4 B**). The effect on  $C_i$  affinity was observed only when myxothiazol and SHAM were added together (**Extended data Fig. 8**), indicating that both alternative oxidase and cytochrome *bc<sub>1</sub>* electron pathways contribute to CCM energization. Importantly, respiratory inhibitors also increased the  $K_{1/2}$  of air-grown *bsti-1* mutant (**Fig. 4 B, Extended data Fig. 7 H**), thus showing that the contribution of mitochondria to CCM energization operates at the level of other transporters than thylakoidal BSTs. The contribution of the different pathways (CEF, PCEF and CMEF) was deduced from  $\text{O}_2$  consumption rates measured in the different mutants during  $C_i$  depletion (**Extended data Fig. 6**). While the contribution of CEF remained relatively constant, the contribution of FLV-mediated PCEF and of CMEF dramatically increased at low  $C_i$  (**Fig. 5 A**).

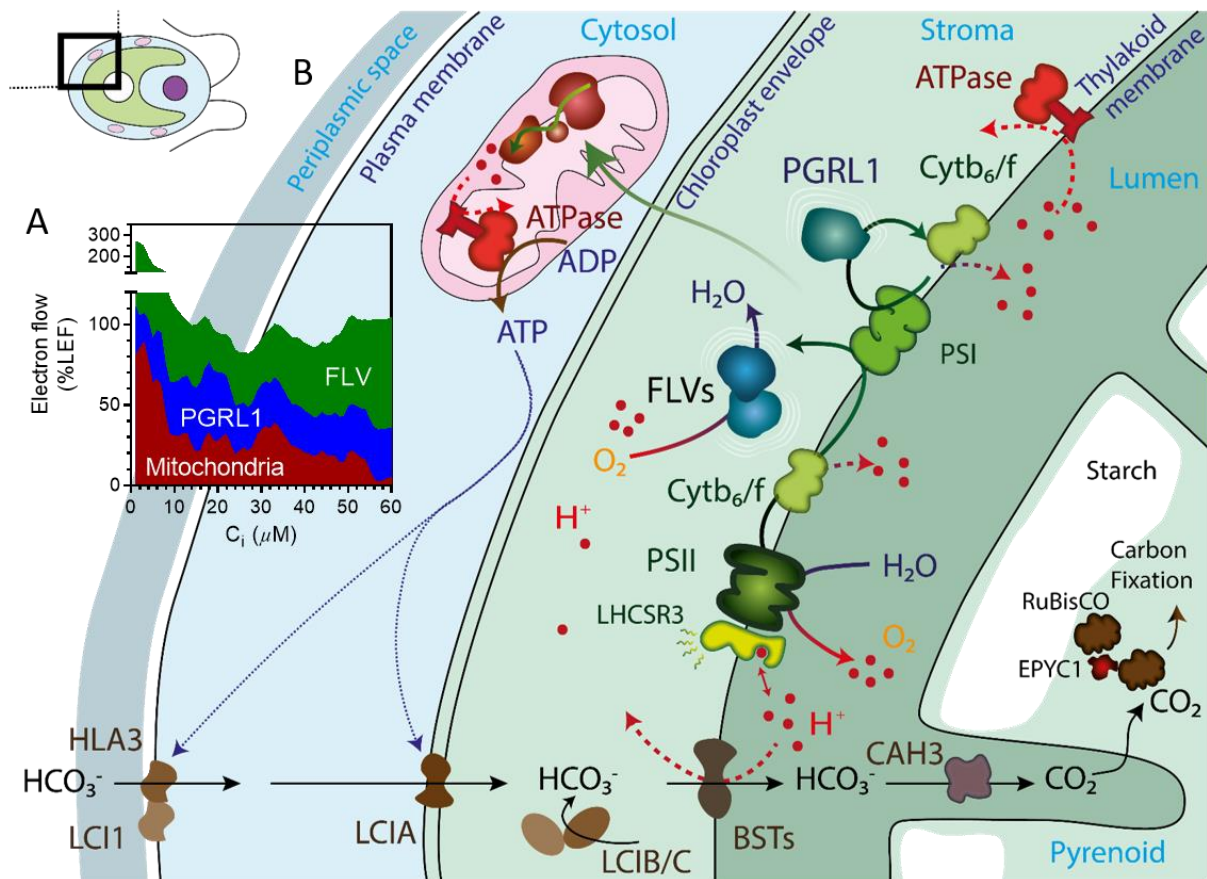


**Figure 5. Proposed mechanism of CCM energization network in algal cells.** (A) The relative contribution of FLV-mediated PCEF, PGRL1-mediated CEF and CMEF to CCM energization at different  $C_i$  concentrations are quantified from  $\text{O}_2$  exchange measurements performed in the different mutant strains and expressed as a percentage of LEF (**Extended data Fig. 6**). (B) Schematic view of the energy supply network to the CCM. CCM components including LCI1, HLA3, LCIA and BSTs transporters, LCIB, LCIC, CAH3, EYPC1 and RuBisCO are shown in brown, and components of the photosynthetic electron transport chain (PSII, PSI, Cytb<sub>6/f</sub>) in green. We propose here that energization of BSTs-dependent  $C_i$  transport is mediated by the *pmf* produced by the combined action of FLVs-mediated  $\text{O}_2$  photoreduction and the PGRL1-mediated cyclic electron flow. CMEF would generate the ATP needed to power other cellular  $C_i$  transporters such as LCIA and HLA3.

## Discussion

Although the CCM's requirement for photosynthesis energy has been early recognized<sup>15</sup>, the associated molecular mechanisms have remained poorly understood<sup>4</sup>. The participation of PCEF<sup>33</sup> or CEF<sup>34</sup> has been proposed, but their actual and respective contributions have not been established. In this work, we demonstrate that both FLV-mediated PCEF and PGRL1-mediated CEF cooperate to supply energy to the CCM. Moreover, we show that the trans-thylakoidal *pmf* generated by both mechanisms is the energy vector used by the recently discovered trans-thylakoidal BST-like  $C_i$  transporters<sup>14</sup>.

We further establish that mitochondrial respiration, the role of which in CCM energization has so far been largely ignored, provides energy to other CCM transporters than BSTs, through an efficient inter-organelles redox trafficking. From the analysis of the respective contribution of each mechanism as a function of  $C_i$  concentration, we conclude that while CEF contribution is relatively constant, PCEF contribution increases at low  $C_i$  concentrations, and that contribution of CMEF also becomes important at the lowest  $C_i$  concentrations. Since these are typical conditions where putative ATP-dependent periplasmic and chloroplast envelope transporters (HLA3 and LCIA respectively) are highly active<sup>4,12,13</sup>, we propose that the ATP produced by CMEF at low  $C_i$  supplies energy to one or both transporters (**Fig. 5**). Interestingly, LCII accumulation, whose function is tightly linked to HLA3<sup>3,29</sup>, decreased in *pgrl1*, *flvB*, *pgrl1 flvB* and *bsti-1*, indicating that impairments of  $C_i$  transport at the thylakoid level may regulate periplasmic transport processes mediated by LCII. This could be due to an increased cytosolic  $C_i$  concentration resulting from the absence of functional thylakoid  $C_i$  transport, which would in turn trigger down-regulation of LCII expression to avoid cytosolic  $C_i$  over-accumulation.

The presence of an active CCM is a key factor influencing phytoplankton biomass production in the oceans<sup>2</sup>, especially for phytoplankton species producing large oceanic blooms<sup>35</sup>. However, the lack of knowledge on CCM operation *in situ*<sup>9</sup> makes it difficult to predict how global changes will affect phytoplankton communities<sup>36</sup>. We demonstrate here that the presence of a functional CCM can be probed by measuring  $C_i$ -dependent NPQ, which could be used as a simple parameter to determine CCM activity in aquatic ecosystems. In diatoms which are important in marine ecosystems<sup>37</sup> and well-studied species<sup>38</sup>, FLVs are absent (they are restricted to the green algal lineage), and CEF is working at very low levels<sup>28</sup>, and it was proposed that the ATP requirement of photosynthesis was fulfilled by an efficient chloroplast to mitochondria energy trafficking<sup>28</sup>. Based on the dependence of CCM on mitochondrial respiration observed here, we propose that in diatoms such energy trafficking between

chloroplast and mitochondria could play an important role in fulfilling the ATP requirement of CCM transporters, including BST-like transporters which are well conserved in most microalgal phyla<sup>39</sup>.

A potential limitation of a thylakoid C<sub>i</sub> pump consuming the *pmf* would be competition with the synthesis of ATP required for CO<sub>2</sub> fixation<sup>14</sup>. This is particularly critical since LEF is known to supply less ATP than required for CO<sub>2</sub> fixation<sup>17</sup>. We suggest here that the combined action of the three alternative mechanisms, CEF, PCEF and CMEF, which all result in an increase of the ATP/NADPH ratio, allows to fulfill the energy requirement of the CCM without compromising CO<sub>2</sub> fixation. A major biotechnological challenge in CCM research is the improvement of crop productivity by transferring microalgal components into higher plants<sup>40-42</sup>. Building a fully functional CCM in plants represents a tremendous scientific challenge, which has recently regained considerable interest<sup>4,43</sup>. Our study shows that an integrated understanding of the cellular energetics is key towards fulfilling the energy requirement of a synthetic CCM without compromising the efficiency of photosynthetic CO<sub>2</sub> fixation. For instance, the expression of FLVs in higher plants which has been shown to supply extra *pmf* during photosynthesis<sup>44-47</sup>, appears as a promising starting point to supply the extra energy needed to power thylakoid C<sub>i</sub> transporters of the BST family in plants. We foresee that future research coupling energy source and CCM expression should help boost plant productivity.

### Accession numbers

Genes studied in this article can be found on <https://phytozome.jgi.doe.gov/> under the loci Cre12.g531900 (FLVA), Cre16.g691800 (FLVB), Cre07.g340200 (PGRL1), Cre16.g662600 (BST1), Cre16.g663400 (BST2), and Cre16.g663450 (BST3).

**List of abbreviations.** BST: Bestrophin-like proteins; CCM: Carbon Concentrating Mechanism; CEF: Cyclic Electron Flow; C<sub>i</sub>: Inorganic Carbon; CMEF: Chloroplast-Mitochondria Electron Flow; HLA3: High Light Activated 3; LCI: Low Carbon Induced; LEF: Linear Electron Flow; LHCSR3: Light Harvesting Complex Stress Related 3; Myxo : Myxothiazol; NPQ: Non Photochemical Quenching; PCEF: Pseudo-Cyclic Electron Flow; PGRL1: Proton Gradient Regulation Like-1; FLVs: Flavodiiron proteins; PSI: Photosystem I; PSII: Photosystem II; RuBisCO: Ribulose Bisphosphate Carboxylase Oxygenase; SHAM: Salicyl hydroxamic acid.

## Materials and Methods

*Chlamydomonas flvB*, *pgrl1*, *bsti-1* mutants and their respective wild-type CC-4533, 137AH and D66 were previously described<sup>14,21,26</sup>. All strains were grown phototrophically under moderate light (80  $\mu\text{mol photons m}^{-2} \text{s}^{-1}$ ) in minimal medium either under low CO<sub>2</sub> or high CO<sub>2</sub>. Gas exchange rates were measured using a membrane inlet mass spectrometer<sup>48</sup> and combined NPQ measurements were done as previously described<sup>49</sup>. All replicates shown are biological replicates from independent cultures. Other methods are described in Supplementary Materials and Methods.

## References:

- 1 Field, C. B., Behrenfeld, M. J., Randerson, J. T. & Falkowski, P. Primary production of the biosphere: integrating terrestrial and oceanic components. *Science* **281**, 237-240, doi:10.1126/science.281.5374.237 (1998).
- 2 Mackey, K. R., Morris, J. J., Morel, F. M. & Kranz, S. A. Response of photosynthesis to ocean acidification. *Oceanography* **28**, 74-91, doi:<https://doi.org/10.5670/oceanog.2015.33> (2015).
- 3 Mackinder, L. C. M. *et al.* A spatial interactome reveals the protein organization of the algal CO<sub>2</sub>-concentrating mechanism. *Cell* **171**, 133-147.e114, doi:<https://doi.org/10.1016/j.cell.2017.08.044> (2017).
- 4 Mackinder, L. C. M. The *Chlamydomonas* CO<sub>2</sub>-concentrating mechanism and its potential for engineering photosynthesis in plants. *New Phytol.* **217**, 54-61, doi:10.1111/nph.14749 (2018).
- 5 Raven, J. A. Inorganic carbon acquisition by eukaryotic algae: four current questions. *Phot. Res.* **106**, 123-134, doi:10.1007/s11120-010-9563-7 (2010).
- 6 Raven, J. A., Beardall, J. & Giordano, M. Energy costs of carbon dioxide concentrating mechanisms in aquatic organisms. *Phot. Res.* **121**, 111-124, doi:10.1007/s11120-013-9962-7 (2014).
- 7 Maberly, S. C. & Gontero, B. Ecological imperatives for aquatic CO<sub>2</sub>-concentrating mechanisms. *J. Exp. Bot.* **68**, 3797-3814, doi:10.1093/jxb/erx201 (2017).
- 8 Savir, Y., Noor, E., Milo, R. & Tlusty, T. Cross-species analysis traces adaptation of Rubisco toward optimality in a low-dimensional landscape. *Proc. Nat. Acad. Sci. USA* **107**, 3475-3480, doi:10.1073/pnas.0911663107 (2010).
- 9 Reinfelder, J. R. Carbon concentrating mechanisms in eukaryotic marine phytoplankton. *Annu. Rev. Mar. Sci.* **3**, 291-315, doi:10.1146/annurev-marine-120709-142720 (2011).
- 10 Moroney, J. V. *et al.* The carbonic anhydrase isoforms of *Chlamydomonas reinhardtii*: intracellular location, expression, and physiological roles. *Phot. Res.* **109**, 133-149, doi:10.1007/s11120-011-9635-3 (2011).
- 11 Duanmu, D., Miller, A. R., Horken, K. M., Weeks, D. P. & Spalding, M. H. Knockdown of limiting-CO<sub>2</sub>-induced gene HLA3 decreases HCO<sub>3</sub><sup>-</sup> transport and photosynthetic Ci affinity in *Chlamydomonas reinhardtii*. *Proc. Natl. Acad. Sci. U. S. A.* **106**, 5990-5995, doi:10.1073/pnas.0812885106 (2009).

- 12 Wang, Y. & Spalding, M. H. Acclimation to very low CO<sub>2</sub>: contribution of limiting CO<sub>2</sub> inducible proteins, LCIB and LCIA, to inorganic carbon uptake in *Chlamydomonas reinhardtii*. *Plant Physiol.* **166**, 2040-2050, doi:10.1104/pp.114.248294 (2014).
- 13 Yamano, T., Sato, E., Iguchi, H., Fukuda, Y. & Fukuzawa, H. Characterization of cooperative bicarbonate uptake into chloroplast stroma in the green alga *Chlamydomonas reinhardtii*. *Proc. Nat. Acad. Sci.* **112**, 7315-7320, doi:10.1073/pnas.1501659112 (2015).
- 14 Mukherjee, A. *et al.* Thylakoid localized bestrophin-like proteins are essential for the CO<sub>2</sub> concentrating mechanism of *Chlamydomonas reinhardtii*. *Proc. Nat. Acad. Sci. U. S. A.* **116**, 16915-16920, doi:10.1073/pnas.1909706116 (2019).
- 15 Badger, M. R., Kaplan, A. & Berry, J. A. Internal inorganic carbon pool of *Chlamydomonas reinhardtii*. *Plant Physiol.* **66**, 407-413, doi:10.1104/pp.66.3.407 (1980).
- 16 Allen, J. F. Photosynthesis of ATP—Electrons, Proton Pumps, Rotors, and Poise. *Cell* **110**, 273-276, doi:[https://doi.org/10.1016/S0092-8674\(02\)00870-X](https://doi.org/10.1016/S0092-8674(02)00870-X) (2002).
- 17 Allen, J. F. Cyclic, pseudocyclic and noncyclic photophosphorylation: new links in the chain. *Trends Plant Sci.* **8**, 15-19, doi:10.1016/s1360-1385(02)00006-7 (2003).
- 18 Munekage, Y. *et al.* PGR5 is involved in cyclic electron flow around photosystem I and is essential for photoprotection in *Arabidopsis*. *Cell* **110**, 361-371, doi:[https://doi.org/10.1016/S0092-8674\(02\)00867-X](https://doi.org/10.1016/S0092-8674(02)00867-X) (2002).
- 19 Johnson, X. *et al.* Proton gradient regulation 5-mediated cyclic electron flow under ATP- or redox-limited conditions: a study of  $\Delta$ ATPase *pgr5* and  $\Delta$ rbcL *pgr5* mutants in the green alga *Chlamydomonas reinhardtii*. *Plant Physiol.* **165**, 438-452, doi:10.1104/pp.113.233593 (2014).
- 20 DalCorso, G. *et al.* A complex containing PGRL1 and PGR5 is involved in the switch between linear and cyclic electron flow in *Arabidopsis*. *Cell* **132**, 273-285, doi:10.1016/j.cell.2007.12.028 (2008).
- 21 Tolleter, D. *et al.* Control of hydrogen photoproduction by the proton gradient generated by cyclic electron flow in *Chlamydomonas reinhardtii*. *Plant Cell* **23**, 2619-2630, doi:10.1105/tpc.111.086876 (2011).
- 22 Curien, G. *et al.* The Water to Water Cycles in Microalgae. *Plant Cell Physiol.* **57**, 1354-1363, doi:10.1093/pcp/pcw048 (2016).
- 23 Helman, Y. *et al.* Genes encoding a-type flavoproteins are essential for photoreduction of O<sub>2</sub> in cyanobacteria. *Curr. Biol.* **13**, 230-235 (2003).
- 24 Gerotto, C. *et al.* Flavodiiron proteins act as safety valve for electrons in *Physcomitrella patens*. *Proc. Nat. Acad. Sci. U.S.A.* **113**, 12322-12327, doi:10.1073/pnas.1606685113 (2016).
- 25 Shimakawa, G. *et al.* The Liverwort, *Marchantia*, drives alternative electron flow using a flavodiiron protein to protect PSI. *Plant Physiol.* **173**, 1636-1647, doi:10.1104/pp.16.01038 (2017).
- 26 Chauv, F. *et al.* Flavodiiron proteins promote fast and transient O<sub>2</sub> photoreduction in *Chlamydomonas*. *Plant Physiol.* **174**, 1825-1836, doi:10.1104/pp.17.00421 (2017).
- 27 Dang, K. V. *et al.* Combined increases in mitochondrial cooperation and oxygen photoreduction compensate for deficiency in cyclic electron flow in *Chlamydomonas reinhardtii*. *Plant Cell* **26**, 3036-3050, doi:10.1105/tpc.114.126375 (2014).
- 28 Bailleul, B. *et al.* Energetic coupling between plastids and mitochondria drives CO<sub>2</sub> assimilation in diatoms. *Nature* **524**, 366, doi:10.1038/nature14599 (2015).
- 29 Kono, A. & Spalding, M. H. LCII1, a *Chlamydomonas reinhardtii* plasma membrane protein, functions in active CO<sub>2</sub> uptake under low CO<sub>2</sub>. *Plant J.* **102**, 1127-1141, doi:<https://doi.org/10.1111/tpj.14761> (2020).



- 30 Bonente, G. *et al.* Analysis of LhcSR3, a protein essential for feedback de-excitation in the green alga *Chlamydomonas reinhardtii*. *Plos Biol.* **9**, e1000577, doi:10.1371/journal.pbio.1000577 (2011).
- 31 Tian, L. *et al.* pH dependence, kinetics and light-harvesting regulation of nonphotochemical quenching in *Chlamydomonas*. *Proc Nat. Acad. Sci. USA* **116**, 8320-8325, doi:10.1073/pnas.1817796116 (2019).
- 32 Sültemeyer, D. F., Klug, K. & Fock, H. P. Effect of dissolved inorganic carbon on oxygen evolution and uptake by *Chlamydomonas reinhardtii* suspensions adapted to ambient and CO<sub>2</sub>-enriched air. *Photosynth. Res.* **12**, 25-33, doi:10.1007/BF00019148 (1987).
- 33 Sültemeyer, D., Biehler, K. & Fock, H. P. Evidence for the contribution of pseudocyclic photophosphorylation to the energy requirement of the mechanism for concentrating inorganic carbon in *Chlamydomonas*. *Planta* **189**, 235-242 (1993).
- 34 Lucker, B. & Kramer, D. M. Regulation of cyclic electron flow in *Chlamydomonas reinhardtii* under fluctuating carbon availability. *Photosynthesis Res.* **117**, 449-459, doi:10.1007/s11120-013-9932-0 (2013).
- 35 Rost, B., Riebesell, U., Burkhardt, S. & Sültemeyer, D. Carbon acquisition of bloom-forming marine phytoplankton. *Limnol. Oceano.* **48**, 55-67, doi:<https://doi.org/10.4319/lo.2003.48.1.0055> (2003).
- 36 Basu, S. & Mackey, K. R. M. Phytoplankton as key mediators of the biological carbon pump: their responses to a changing climate. *Sustainability* **10**, doi:10.3390/su10030869 (2018).
- 37 Karlusich, J. J. P., Ibarbalz, F. M. & Bowler, C. Phytoplankton in the tara ocean. *Annu. Rev. Mar. Sci.* **12**, 233-265, doi:10.1146/annurev-marine-010419-010706 (2020).
- 38 Falciatore, A., Jaubert, M., Bouly, J.-P., Bailleul, B. & Mock, T. Diatom molecular research comes of age: model species for studying phytoplankton biology and diversity. *Plant Cell* **32**, 547-572, doi:10.1105/tpc.19.00158 (2020).
- 39 Hennon, G. M. M., Hernández Limón, M. D., Haley, S. T., Juhl, A. R. & Dyrman, S. T. Diverse CO<sub>2</sub>-induced responses in physiology and gene expression among eukaryotic phytoplankton. *Front. Microbiol.* **8**, doi:10.3389/fmicb.2017.02547 (2017).
- 40 Atkinson, N. *et al.* Introducing an algal carbon-concentrating mechanism into higher plants: location and incorporation of key components. *Plant Biotechnol J.* **14**, 1302-1315, doi:10.1111/pbi.12497 (2016).
- 41 Meyer, M. T., McCormick, A. J. & Griffiths, H. Will an algal CO<sub>2</sub>-concentrating mechanism work in higher plants? *Curr. Opin. Plant Biol.* **31**, 181-188, doi:<https://doi.org/10.1016/j.pbi.2016.04.009> (2016).
- 42 Nölke, G. *et al.* The integration of algal carbon concentration mechanism components into tobacco chloroplasts increases photosynthetic efficiency and biomass. *Biotechnol. J.* **14**, 1800170, doi:<https://doi.org/10.1002/biot.201800170> (2019).
- 43 Hennacy, J. H. & Jonikas, M. C. Prospects for engineering biophysical CO<sub>2</sub> concentrating mechanisms into land plants to enhance yields. *Annu. Rev. Plant Biol.* **71**, 461-485, doi:10.1146/annurev-arplant-081519-040100 (2020).
- 44 Yamamoto, H., Takahashi, S., Badger, M. R. & Shikanai, T. Artificial remodelling of alternative electron flow by flavodiiron proteins in Arabidopsis. *Nat. Plants* **2**, 16012, doi:10.1038/nplants.2016.12 (2016).
- 45 Wada, S. *et al.* Flavodiiron protein substitutes for cyclic electron flow without competing CO<sub>2</sub> assimilation. *Plant Physiol.*, doi:10.1104/pp.17.01335 (2017).
- 46 Gómez, R. *et al.* Faster photosynthetic induction in tobacco by expressing cyanobacterial flavodiiron proteins in chloroplasts. *Photosynth. Res.* **136**, 129-138, doi:10.1007/s11120-017-0449-9 (2018).

- 47 Vicino, P. *et al.* Expression of flavodiiron proteins Flv2-Flv4 in chloroplasts of *Arabidopsis* and tobacco plants provides multiple stress tolerance. *Int. J. Mol. Sci.* **22**, 1178 (2021).
- 48 Burlacot, A., Burlacot, F., Li-Beisson, Y. & Peltier, G. Membrane Inlet Mass Spectrometry: A Powerful Tool for Algal Research. *Front. Plant. Sci.* **11**, doi:10.3389/fpls.2020.01302 (2020).
- 49 Burlacot, A. *et al.* Flavodiiron-mediated O<sub>2</sub> photoreduction links H<sub>2</sub> production with CO<sub>2</sub> fixation during the anaerobic induction of photosynthesis. *Plant Physiol.* **177**, 1639-1649, doi:10.1104/pp.18.00721 (2018).

### Acknowledgments:

This work was supported by the A\*MIDEX (ANR-11-IDEX-0001-02) project and by the ANR OTOLHYD. Ousmane Dao is the recipient of a PhD grant awarded to Y. L-B. The authors thank Pr. Graham Peers for stimulating discussion, Pr. Krishna K. Niyogi and Dr. Masakazu Iwai for critical reading of the manuscript, Pr. James V. Moroney for providing the *bsti-1* mutant, Pr. Luke Mackinder and Pr. Hideya Fukuzawa for respectively providing BST3, and LCIA, LCII antibodies. Contributions of Dr. Solène Moulin for artistic drawings of Fig. 5, of Stephanie Blangy for LCIC antibody preparation, Emma Calikanzaros for preliminary experiments and Arthur Gosset for performing genetic crosses of *flvB* and *pgrl1* mutant, are gratefully acknowledged. The authors acknowledge the European Union Regional Developing Fund, the Region Provence Alpes Côte d'Azur, the French Ministry of Research, and the CEA for funding the HelioBiotec platform.

**Competing interests:** The authors declare that they have no competing interest.

**Data and materials availability:** All data needed to evaluate the conclusions in the paper are present in the paper and/or the Supplementary Materials.

### List of Figures:

**Figure 1. Affinity of photosynthetic O<sub>2</sub> evolution for inorganic carbon (C<sub>i</sub>) is decreased in *pgrl1 flvB* double mutants, but unaffected in *flvB* and *pgrl1* single mutants.** Net O<sub>2</sub> production was measured at pH 7.2 in cells grown under 400 ppm CO<sub>2</sub> air (Low CO<sub>2</sub>) (**A, B and C**) or 3% CO<sub>2</sub> (High CO<sub>2</sub>) (**D, E and F**). Shown are three replicates for each strain (dots) and hyperbolic fit with variability (plain lines, dotted lines). For each replicate, net O<sub>2</sub> production was measured following stepwise C<sub>i</sub> addition, and normalized to the maximum

photosynthetic net O<sub>2</sub> production. Since these strains were generated in different genetic backgrounds (CC-4533 and 137AH, respectively) showing contrasted photosynthetic activities (**Extended data Fig. 2 A, C**), data shown are normalized to the maximal net O<sub>2</sub> production rate. (**A, D**) 137AH and CC-4533 are the respective control strains for *pgrl1* and *flvB*, WT-1 to -4 are four independent control strains obtained from the *pgrl1* × *flvB* crossing. (**B, E**) *flvB* and *pgrl1* mutant strains. (**C, F**) *pgrl1 flvB*-1 to -5 are five independent double mutant strains. **G** Immunodetection of PGRL1, FLVA and FLVB in the different strains with Coomassie blue staining as the loading control. (**H**) K<sub>1/2</sub> values as determined from the hyperbolic fit for each strain. Shown are mean ± SD (n=3 for single mutants and their controls), values for all double mutant strains have been pooled (“*pgrl1 flvB* all”, n=15) as well as their control strains (“WT all”, n=12). Asterisks represent significant differences (p<0.05, one way ANOVA with Tukey correction).

**Figure 2. Growth of *pgrl1 flvB* double mutants is impaired at low CO<sub>2</sub> while CCM components are present.** (**A**). Growth tests performed on *pgrl1*, *flvB*, and their corresponding control strains (137AH and CC-4533 respectively) (left panels) and on double mutants (*pgrl1 flvB*-1 to -5) and their control strains (WT-1 to -4) (right panels); the CCM1 mutant *cia5* was introduced as a CCM-deficient control together with its reference strain CC-125. Cells were spotted on plates containing minimal medium at pH 7.2 and grown under continuous illumination (60 μmol photon m<sup>-2</sup> s<sup>-1</sup>) either under High CO<sub>2</sub>, Low CO<sub>2</sub> or Very Low CO<sub>2</sub> (100 ppm CO<sub>2</sub> in air). Shown are representative spots of ten independent experiments. (**B**) Immunodetection of PGRL1, FLVA, FLVB and of the major CCM components in two independent *pgrl1 flvB* double mutants and controls grown in Low CO<sub>2</sub> or High CO<sub>2</sub>. (**C**) Carbonic anhydrase (CA) activity was determined *in vivo* by following the unlabelling of <sup>18</sup>O-enriched CO<sub>2</sub> in the same strains and conditions as in **B**. Shown are mean values and replicates (n=3).

**Figure 3. The NPQ dependence to C<sub>i</sub> concentration is abolished in *pgrl1 flvB* double mutants and in the BST mutant *bsti-1*.** (**A**) Schematic view describing the rationale of the experiment; NPQ, which depends on the luminal pH (via LHCSR3) is used to probe the trans-thylakoidal *pmf* during the CCM functioning. (**B-E**) Combined measurements of chlorophyll fluorescence (upper panels), C<sub>i</sub> concentrations and NPQ (lower panels) during dark-light-dark transients in WT-2 (**B**), *pgrl1 flvB*-3 (**C**), the *bsti-1* control strain D66 (**D**) and *bsti-1* (**E**). All

strains were grown at low CO<sub>2</sub>. Shown are representative experiments (n=3). Red arrows indicate addition of bicarbonate.

**Figure 4. Mitochondrial inhibitors decrease the affinity of photosynthesis for C<sub>i</sub> in low CO<sub>2</sub>-grown cells.** Photosynthetic net O<sub>2</sub> production was measured as in **Fig. 1** in High CO<sub>2</sub> (**A**) or Low CO<sub>2</sub> (**B**) grown cells. K<sub>1/2</sub> values were determined from hyperbolic fits in the different strains in the presence or absence of two mitochondrial inhibitors myxothiazol (Myxo, 2.5 μM) and salicyl hydroxamic acid (SHAM, 400 μM), respectively acting on the cytochrome *bc<sub>1</sub>* complex and on the alternative oxidase. Shown are mean values (n=3, ±SD). All strains showed K<sub>1/2</sub> significantly different when treated with myxothiazol and SHAM as compared to their control when grown in low CO<sub>2</sub> (p<0.05; one way ANOVA with Tukey correction).

**Figure 5. Proposed mechanism of CCM energization network in algal cells.** (**A**) The relative contribution of FLV-mediated PCEF, PGRL1-mediated CEF and CMEF to CCM energization at different C<sub>i</sub> concentrations are quantified from O<sub>2</sub> exchange measurements performed in the different mutant strains and expressed as a percentage of LEF (**Extended data Fig. 6**). (**B**) Schematic view of the energy supply network to the CCM. CCM components including LCI1, HLA3, LCIA and BSTs transporters, LCIB, LCIC, CAH3, EYPC1 and RuBisCO are shown in brown, and components of the photosynthetic electron transport chain (PSII, PSI, Cytb<sub>6</sub>/f) in green. We propose here that energization of BSTs-dependent C<sub>i</sub> transport is mediated by the *pmf* produced by the combined action of FLVs-mediated O<sub>2</sub> photoreduction and the PGRL1-mediated cyclic electron flow. CMEF would generate the ATP needed to power other cellular C<sub>i</sub> transporters such as LCIA and HLA3.